Inorganic Chemistry

COMMUNICATION

pubs.acs.org/IC

Steric Effects Control Self-Sorting in Self-Assembled Clusters

Amber M. Johnson and Richard J. Hooley*

Department of Chemistry, University of California at Riverside, Riverside, California 92521, United States

Supporting Information

ABSTRACT: Endohedrally functionalized bis(pyridine) ligands show the ability to self-discriminate when treated with coordinating metals to form self-assembled clusters. Self-sorting between components is controlled by substitution on the *interior* of the complex. Tuning the size of the internal substituent allows selective heterocluster formation, determined by noncovalent and space-filling interactions. This novel method of self-sorting allows discrimination between ligands of identical geometry and donor type.

The self-sorted noncovalent assembly of individual components is commonplace and essential in biological systems, most notably in cDNA base-pair attraction.[1] These principles have been applied to synthetic systems,[2] and a number of examples of self-sorting behavior are known. These often exploit complementary hydrogen-bonding motifs[3] or specific receptor−substrate interactions.[4] In each case, a "lock-and-key" motif is favored, whereby different components show preferential affinity for each other through specific complementary contacts.[5]

Self-assembled metal−ligand clusters have a variety of uses such as synthetic hosts, enzyme mimics, and functional materials.[6] Self-sorting behavior can be observed in the noncovalent self-assembly of metallosupramolecules, utilizing a variety of metal−ligand contacts as structural vertices.[7] In these cases, geometrical constraints are used to favor the formation of one complex over another. The ability to control the assembly of differently functionalized components with the *same* geometry and identical coordination motifs would greatly expand the scope and utility of these complexes. In order to achieve this, the ligands must contain a structural element that allows for differentiation between components. This can be provided by endohedral derivatization of the ligands. Internally functionalized metal−ligand clusters are relatively rare and are generally two-dimensional (2D) polygons[8] and large supercapsules.[9] Here we report noncovalent self-sorting of metal−ligand clusters controlled solely by steric effects between endohedrally functionalized ligands.

Recently, we reported a self-assembled palladium pyridyl "paddle-wheel" M_2L_4 cluster system that displays a defined cavity and host behavior in organic solvents.[10] Ligand **1a** self-assembles into the structure shown in Figure 1 upon the addition of weakly ligated palladium(II) salts. The initial formation of the complex is extremely rapid, and EXSY NMR experiments showed no exchange of components on the NMR time scale. Crystallographic analysis of $\mathbf{1a_4 \cdot Pd_2}$ shows that the cavity measures 11.8 Å × 8.5 Å in the solid state,[10] suggesting that internally positioned substituents of the correct size would allow control of the self-assembly through steric effects. Internally derivatized amine ligand **1b** was synthesized via Sonogashira coupling of 2,6-dibromoaniline and 3-ethynylpyridine (see the Supporting Information). Molecular modeling of the cluster $\mathbf{1b_4 \cdot Pd_2}$ shows no steric clash between the amines, and so larger substituents were targeted from this scaffold. The amine in **1b** is poorly nucleophilic, but reaction with trifluoroacetic anhydride or phenylisocyanate was possible, giving "medium-sized" acetate **1c** and "large" urea **1d**, respectively.

As expected, amine ligand **1b** self-assembled into the requisite cluster upon treatment with $Pd(NO_3)_2$ in DMSO-d_6 (Figure 2b). The larger trifluoroacetate ligand **1c**, however, did not show any self-assembly. A broad, unidentifiable NMR spectrum was observed, with no precipitation from the solution. Molecular modeling of the $\mathbf{1c_4 \cdot Pd_2}$ complex suggests that the introversion of four trifluoroacetamide (TFA) groups is sterically impossible, and so the M_2L_4 cluster cannot form. The ligand is not free in solution but probably forms undefined Pd−L aggregate mixtures.[11]

Self-sorting was tested by combining ligands **1a**, **1b**, and **1c** with $Pd(NO_3)_2$ in DMSO-d_6. The formation of the clusters is extremely rapid, and upon mixing ligands **1a** and **1b** (1:1) at room temperature with 0.5 mol equiv of $Pd(NO_3)_2$, a complex NMR spectrum was observed (see Figure 2d). No peaks for either ligand remained, indicating complete cluster formation. The spectrum, while complex, was sharp, and most of the peaks were well-defined. Partial interpretation was possible by altering the proportions of **1a** and **1b** used. The region of the ^{1}H NMR spectrum corresponding to protons H_1 was the clearest and so was used for identification (Figure 3). A comparison of the heterocluster spectrum with the $\mathbf{(1a)_4 \cdot Pd_2}$ and $\mathbf{(1b)_4 \cdot Pd_2}$ spectra allowed for identification of the peaks (labeled in red and blue, respectively) of those homoclusters. Heteroclusters were identified by mixing the component ligands in a 3:1 ratio to enhance the corresponding 3:1 heterocluster peaks. When 3 equiv of **1a** and 1 equiv of **1b** were combined, three peaks were prominent and assigned as $\mathbf{(1a)_4 \cdot Pd_2}$ and $\mathbf{(1a)_3 \cdot 1b \cdot Pd_2}$. In the opposite mixture ($1\times$**1a**:$3\times$**1b**), different peaks were enhanced, and these were assigned as $\mathbf{(1b)_4 \cdot Pd_2}$ and $\mathbf{1a \cdot (1b)_3 \cdot Pd_2}$. Clear identification of the two $\mathbf{(1a)_2 \cdot (1b)_2 \cdot Pd_2}$ isomers was not possible. A 2D NOESY spectrum was unhelpful in this case because of the large number of peaks in the H_1 region with similar δ.

To determine whether the self-assembly was kinetically or thermodynamically controlled, $Pd(NO_3)_2$ was titrated into a 1:1 mixture of **1a** and **1b** (see the Supporting Information, Figure S-1). As the proportion of Pd^{2+} was increased, the distribution of isomers in the cluster mixture remained identical. No change in the ligand distribution occurred over time, and so the cluster

Received: January 24, 2011
Published: April 25, 2011

 © 2011 American Chemical Society dx.doi.org/10.1021/ic2001688 | *Inorg. Chem.* 2011, 50, 4671–4673

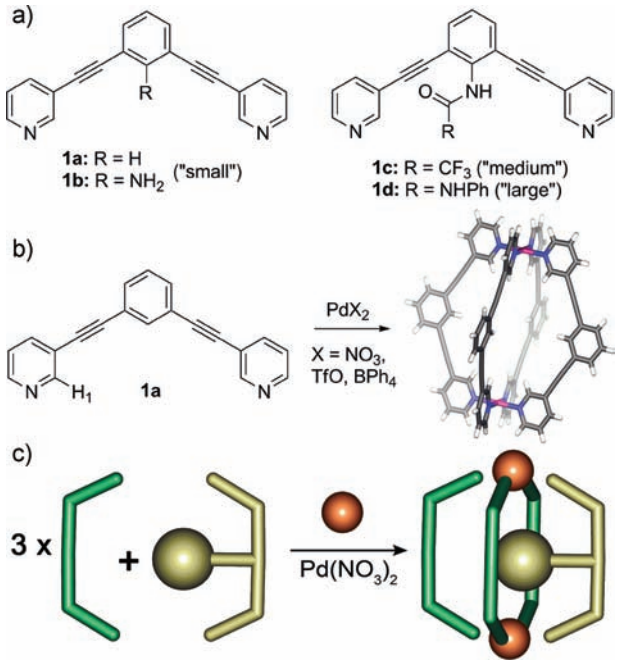

Figure 1. (a) Ligands used in this study. (b) Self-assembly of M_2L_4 "paddle-wheel" cluster $\mathbf{1a}_4\cdot\mathbf{Pd}_2$.[10] (c) Self-sorting through steric effects.

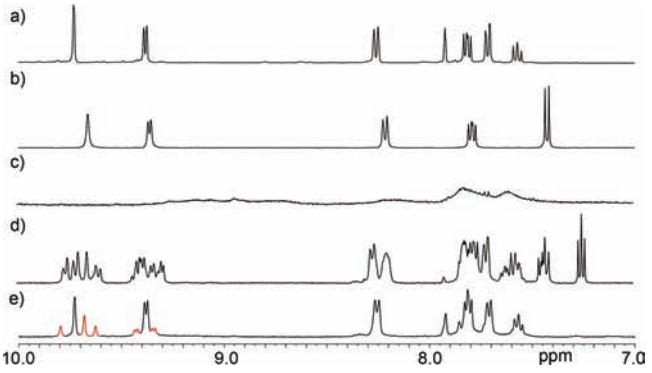

Figure 2. ^{1}H NMR spectra of self-sorted cluster formation (4 mM, 400 MHz, DMSO-d_6, 300 K): (a) cluster $\mathbf{1a}_4\cdot\mathbf{Pd}_2$; (b) cluster $\mathbf{1b}_4\cdot\mathbf{Pd}_2$; (c) cluster $\mathbf{1c}_4\cdot\mathbf{Pd}_2$; (d) a mixture of "small" ligands **1a**, **1b**, and $Pd(NO_3)_2$ (2:2:1), $\mathbf{1b}_4\cdot\mathbf{Pd}_2$; (e) a mixture of "small" and "medium" ligands **1a**, **1c**, and $Pd(NO_3)_2$ (6:2:1). Peaks from $(\mathbf{1a})_3\cdot\mathbf{1c}\cdot\mathbf{Pd}_2$ are labeled in red.

mixture appears to be both the kinetically and thermodynamically favorable product.

When **1a** was combined with trifluoroacetate ligand **1c** and $Pd(NO_3)_2$, however, a much different picture emerged (Figure 2e). No broad peaks were seen, and all ligands present formed M_2L_4 clusters. In this case, only two complexes are seen: the $(\mathbf{1a})_4\cdot\mathbf{Pd}_2$ cluster and the $(\mathbf{1a})_3\cdot\mathbf{1c}\cdot\mathbf{Pd}_2$ cluster. A 2D ROESY spectrum (see the Supporting Information, Figure S-2) allowed identification of the different H_1 resonances for the $(\mathbf{1a})_3\cdot\mathbf{1c}\cdot\mathbf{Pd}_2$ cluster. Small NOE cross peaks were seen between the three peaks denoted in red in Figure 2e. The integral ratio of 1:2:1 corroborates the symmetry of the molecule. The formation of the self-sorted complex was extremely rapid (<30 s), and no change was observed over a 48 h time period. The ligand-exchange process occurs over a period of hours at room temperature (vide infra),

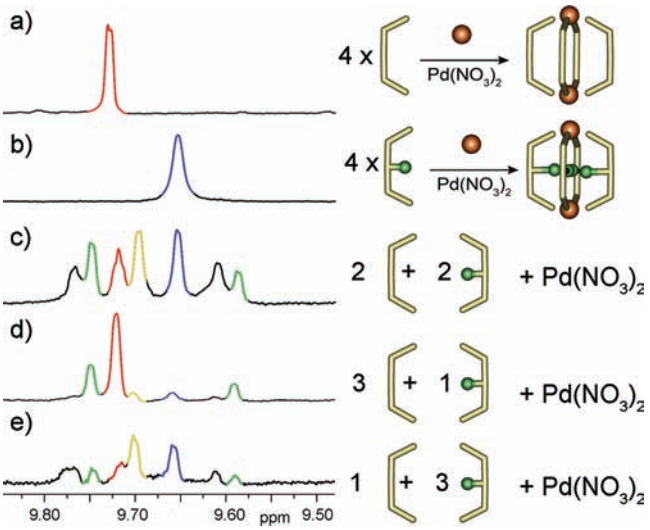

Figure 3. Identification of cluster peaks by ^{1}H NMR of proton H_1 (4 mM, 400 MHz, DMSO-d_6, 300 K). Red: $(\mathbf{1a})_4\cdot\mathbf{Pd}_2$. Blue: $(\mathbf{1b})_4\cdot\mathbf{Pd}_2$. Green: $(\mathbf{1a})_3\cdot\mathbf{1b}\cdot\mathbf{Pd}_2$. Yellow: $\mathbf{1a}\cdot(\mathbf{1b})_3\cdot\mathbf{Pd}_2$. Peaks from $(\mathbf{1a})_2\cdot(\mathbf{1b})_2\cdot\mathbf{Pd}_2$ overlap are labeled in black.

so this indicates the thermodynamic and kinetic stability of the self-sorting.

The "large" urea ligand **1d** was synthesized to test the limits of self-sorting; the endohedral group in **1d** is too large to fit in the $(\mathbf{1a})_4\cdot\mathbf{Pd}_2$ homocluster and is also too large to fit in a 1:3 heterocluster (e.g., $(\mathbf{1a})_3\cdot\mathbf{1d}\cdot\mathbf{Pd}_2$). Upon mixing **1d** with $Pd(NO_3)_2$ in DMSO-d_6, a broad, undefined spectrum was observed that was similar to that seen in Figure 2c. When ligands **1a** and **1d** were mixed, a complex spectrum was observed (see the Supporting Information, Figure S-3). The initial spectrum shows a disordered aggregate of ligand−palladium species. This kinetic mixture is not the thermodynamic product, however. After 48 h, the system reached equilibrium, showing formation of the $(\mathbf{1a})_4\cdot\mathbf{Pd}_2$ cluster, along with broad peaks for $\mathbf{1d}\cdot\mathbf{Pd}$ aggregates. Formation of the paddle-wheel complex in this case is not kinetically favorable but thermodynamically so. Ligand-exchange processes occur on the order of minutes to hours at room temperature. In a similar vein, a combination of the amine and TFA ligands **1b** and **1c** did not show initial cluster formation, but cluster $(\mathbf{1b})_4\cdot\mathbf{Pd}_2$ could be observed after 1 h of mixing. No heteroclusters were observed (see the Supporting Information, Figure S-4).

To confirm the assignment of the NMR spectra, the clusters were subjected to mass spectrometric (MS) analysis under mild ionization conditions with acetonitrile solutions of the clusters (triflate salts). The triflate salts were used for MS analysis because of their solubility in acetonitrile; analysis of DMSO solutions of the nitrate salts was unsurprisingly unsuccessful.[12] Electrospray ionization (ESI) analysis of the $\mathbf{1a}\cdot\mathbf{1b}\cdot\mathbf{Pd}$ mixture showed five clusters of M^+ peaks (Figure 4a). Each of these peaks displays the isotope pattern for the presence of two Pd atoms. There are six statistical possibilities for heterocluster formation in this system, and all are observed (there are two possible coordination geometries for $(\mathbf{1a})_2\cdot(\mathbf{1b})_2\cdot\mathbf{Pd}_2$). Statistical distribution is not observed, however. $(\mathbf{1a})_3\cdot\mathbf{1b}\cdot\mathbf{Pd}_2\cdot\mathbf{OTf}_3$ is favored (ratio $\mathbf{1a}_4$:$\mathbf{1a}_3\mathbf{1b}$:$\mathbf{1a}\mathbf{1b}_3$ = 1:4:2) because of the slight difference in the donor ability between ligands. The relative distributions of the six different clusters are, within error, similar to those seen in the ^{1}H NMR spectrum, favoring $(\mathbf{1a})_3\cdot\mathbf{1b}\cdot\mathbf{Pd}_2$.

dx.doi.org/10.1021/ic2001688 |*Inorg. Chem.* 2011, 50, 4671–4673

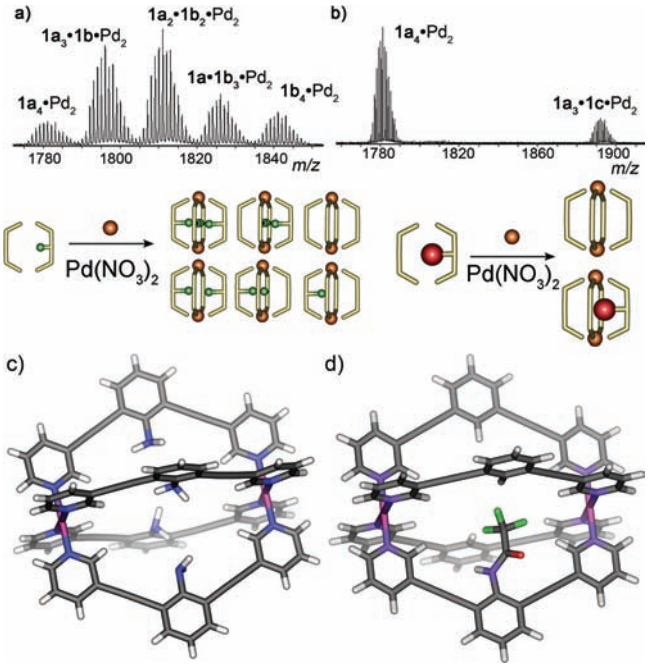

Figure 4. ESI-MS spectra of (a) $\mathbf{1a_3 \cdot 1b \cdot Pd_2 \cdot OTf_3}$ and (b) $\mathbf{1a_3 \cdot 1c \cdot Pd_2 \cdot OTf_3}$ and cartoons of the product mixtures. Molecular minimization of (c) cluster $\mathbf{1b_4 \cdot Pd_2}$ and (d) cluster $\mathbf{1a_3 \cdot 1c \cdot Pd_2}$ (SPARTAN, AM1 force field).[13].

On the other hand, ESI analysis of **1a · 1c · Pd** shows a far more simple spectrum. Only two species are observed, corresponding to the $\mathbf{(1a)_4 \cdot Pd_2 \cdot OTf_3}$ cluster and the $\mathbf{(1a)_3 \cdot 1c \cdot Pd_2 \cdot OTf_3}$ cluster. The selectivity is absolute, and mirrors are observed in the NMR analysis (both the relative intensity of the MS peaks and the integrals in the ^{1}H NMR show a ratio of ~3:1). MS analysis of the "large" complexes was more difficult, however. When the **1a · 1d · Pd** and **1b · 1c · Pd** triflate complexes were analyzed, the only peaks observed were for $\mathbf{(1a)_4 \cdot Pd_2 \cdot OTf_3}$ and $\mathbf{(1b)_4 \cdot Pd_2 \cdot OTf_3}$, respectively. The nonspecific aggregates observed in the NMR are evidently not stable under the ESI-MS conditions and are not observed. No peaks for intact heteroclusters were seen, as expected.

Molecular modeling provides an explanation for the aggregate formed. The TFA group is forced into the interior cavity of the host, filling the space inside (Figure 4d). The TFA occupies over half of the space inside, and there is a distinct steric clash between two endohedral groups, disfavoring the formation of further clusters with endohedral substituents. The phenylurea substituent is too large to favor either homo- or heterocluster formation at all.

In conclusion, we have shown that self-sorting of the noncovalent self-assembly of ligands with identical coordination geometries can be controlled solely by the steric effects of substituents positioned on the interior of the target cluster. Further analysis of methods to control the self-assembly processes are underway in our laboratory.

■ ASSOCIATED CONTENT

Supporting Information. Synthetic procedures and selected NMR data. This material is available free of charge via the Internet at http://pubs.acs.org.

■ AUTHOR INFORMATION

Corresponding Author
*E-mail: richardh@ucr.edu.

■ ACKNOWLEDGMENT

We are grateful to the University of California at Riverside for financial support, and the authors thank Prof. Ryan R. Julian, Erik R. Knudsen, and Dr. Ron New for advice and MS analysis.

■ REFERENCES

(1) Sessler, J. L.; Lawrence, C. M.; Jayawickramarajah, J. *Chem. Soc. Rev.* **2007**, *36*, 341–325.

(2) (a) Krämer, R.; Lehn, J. M.; Marquis-Rigault, A. *Proc. Natl. Acad. Sci. U.S.A.* **1993**, *90*, 5394–5398. (b) Sarma, R. J.; Nitschke, J. R. *Angew. Chem., Int. Ed.* **2008**, *47*, 377–380.

(3) (a) Park, T.; Todd, E. M.; Nakashima, S.; Zimmerman, S. C. *J. Am. Chem. Soc.* **2005**, *127*, 18133–18142. (b) Wu, A. X.; Isaacs, L. *J. Am. Chem. Soc.* **2003**, *125*, 4831–4835.

(4) (a) Mukhopadhyay, P.; Zavalij, P. Y.; Isaacs, L. *J. Am. Chem. Soc.* **2006**, *128*, 14093–14102. (b) Jiang, W.; Schäfter, A.; Mohr, P. C.; Schalley, C. A. *J. Am. Chem. Soc.* **2010**, *132*, 2309–2320. (c) Ghosh, S.; Wu, A. X.; Fettinger, J. C.; Zavalij, P. Y.; Isaacs, L. *J. Org. Chem.* **2008**, *73*, 5915–5925.

(5) (a) Ajami, D.; Hou, J. L.; Dale, T. J.; Barrett, E.; Rebek, J., Jr. *Proc. Natl. Acad. Sci. U.S.A.* **2009**, *106*, 10430–10434. (b) Rowan, S. J.; Hamilton, D. G.; Brady, P. A.; Sanders, J. K. M. *J. Am. Chem. Soc.* **1997**, *119*, 2578–2579.

(6) (a) Fiedler, D.; Leung, D. H.; Bergman, R. G.; Raymond, K. N. *Acc. Chem. Res.* **2005**, *38*, 351–360. (b) Baxter, P.; Lehn, J.-M.; DeCian, A. *Angew. Chem., Int. Ed. Engl.* **1993**, *32*, 69–72. (c) Fujita, M.; Umemoto, K.; Yoshizawa, M.; Fujita, N.; Kusukawa, T.; Biradha, K. *Chem. Commun.* **2001**, 509–518. (d) Leininger, S.; Olenyuk, B.; Stang, P. J. *Chem. Rev.* **2000**, *100*, 853–908.

(7) (a) Northrop, B. H.; Zheng, Y.-R.; Chi, K.-W.; Stang, P. J. *Acc. Chem. Res.* **2009**, *42*, 1554–1563. (b) Zhao, L. Z.; Northrop, B. H.; Zheng, Y.-R.; Yang, H.-B.; Lee, H. J.; Lee, Y. M.; Park, J. Y.; Chi, K.-W.; Stang, P. J. *J. Org. Chem.* **2008**, *73*, 6580–6586. (c) Zheng, Y.-R.; Stang, P. *J. Am. Chem. Soc.* **2009**, *131*, 3487–3489. (d) Schmittel, M.; Mahata, K. *Chem. Commun.* **2010**, *46*, 4163–4165. (e) Mahata, K.; Schmittel, M. *J. Am. Chem. Soc.* **2009**, *131*, 16544–16554. (f) Sun, Q. F.; Iwasa, J.; Ogawa, D.; Ishido, Y.; Sato, S.; Ozeki, T.; Sei, Y.; Yamaguchi, K.; Fujita, M. *Science* **2010**, *328*, 1144–1147. (g) Chand, D. K.; Biradha, K.; Fujita, M. *Chem. Commun.* **2001**, 1652–1654.

(8) Zhao, L.; Ghosh, K.; Zheng, Y.-R.; Stang, P. J. *J. Org. Chem.* **2009**, *74*, 8516–8521.

(9) (a) Sato, S.; Iida, J.; Suzuki, K.; Kawano, M.; Ozeki, T.; Fujita, M. *Science* **2006**, *313*, 1273–1276. (b) Suzuki, K.; Iida, J.; Sato, S.; Kawano, M.; Fujita, M. *Angew. Chem., Int. Ed.* **2008**, *47*, 5780–5782. (c) Suzuki, K.; Kawano, M.; Sato, S.; Fujita, M. *J. Am. Chem. Soc.* **2007**, *129*, 10652–10653. (d) Sato, S.; Ishido, Y.; Fujita, M. *J. Am. Chem. Soc.* **2009**, *131*, 6064–6065.

(10) Liao, P.; Langloss, B. W.; Johnson, A. M.; Knudsen, E. R.; Tham, F. S.; Julian, R. R.; Hooley, R. J. *Chem. Commun.* **2010**, *46*, 4932–4934.

(11) Kim, H.-J.; Lee, E.; Kim, M. G.; Kim, M.-C.; Lee, M.; Sim, E. *Chem.—Eur. J.* **2008**, *14*, 3883–3888.

(12) The NMR spectra of the Pd_2L_4OTf salts were similar to the nitrate spectra shown; $Pd(NO_3)_2$ was used for NMR analysis because of the increased ease of handling.

(13) Dewar, M. J. S.; Zoebisch, E. G.; Healy, E. F.; Stewart, J. J. P. *J. Am. Chem. Soc.* **1985**, *107*, 3902–3909. Calculations were performed on *SPARTAN 06*, Wavefunction Inc.